2 April 1999

Chemical Physics Letters 303 (1999) 27–36

CHEMICAL PHYSICS LETTERS

Gibbs ensemble computer simulation and SAFT-VR theory of non-conformal square-well monomer–dimer mixtures

Clare McCabe [a], Alejandro Gil-Villegas [a,b], George Jackson [c,*]

[a] *Department of Chemistry, University of Sheffield, Sheffield, S3 7HF, UK*
[b] *Instituto de Física, Universidad de Guanajuato, León 37150, Mexico*
[c] *Department of Chemical Engineering and Chemical Technology, Imperial College of Science, Technology and Medicine, Prince Consort Road, London, SW7 2BY, UK*

Received 30 September 1998; accepted 18 January 1999

Abstract

The phase equilibria of non-conformal square-well monomer–dimer systems are examined using Gibbs ensemble Monte Carlo simulation and compared with results from the statistical associating fluid theory for potentials of variable attractive range (SAFT-VR). For the first system of interest the square-well segments are of equal diameter and well-depth, the monomer has an attractive range of $\lambda_{11} = 1.25$ and the dimer of $\lambda_{22} = 1.5$. Two constant-pressure slices of the phase diagram are determined from Gibbs ensemble simulation of the mixture for a range of temperatures. The second system is a united-atom model of the real system methane + *n*-butane which has been extensively studied with SAFT-VR theory; parameters from the theoretical work are used in the simulation. Constant-pressure and -temperature slices are studied and comparisons made between theoretical predictions and simulation data. We extrapolate the mixture simulation data to estimate the pure component phase equilibria.

1. Introduction

The Gibbs ensemble Monte Carlo (GEMC) technique [1] is now generally accepted as a standard method for the simulation of phase equilibria; by using two simulation cells it allows the direct simulation of phase equilibria and eliminates the interfacial problems that arise from conventional single cell methods. This method of simulation also enables closer approach to the critical point due to the possibility of density and composition fluctuations. The Gibbs ensemble has already been used to study the phase equilibria of a wide range of fluids and fluid mixtures; for full details see reviews [1–3].

In this work the GEMC method has been used in the direct simulation of phase equilibria for non-conformal square-well monomer–dimer systems. We report simulation results for two square-well monomer–dimer binary mixtures. In the first mixture the monomer and dimer segments are identical in terms of particle size and well depth but differ in the range of the square-well potential (system I); this enabled us to examine the non-conformal nature of the monomer and dimer mixture interacting through potentials of different range. The second mixture is a model of the real alkane system methane + *n*-butane

* Corresponding author. E-mail: g.jackson@ic.ac.uk

0009-2614/99/$ - see front matter
PII: S0009-2614(99)00104-9

(system II) which has been studied extensively in earlier work [4] with the statistical associating fluid theory for potentials of variable range (SAFT-VR) [5,6] (system II).

SAFT is a molecular based equation of state derived from thermodynamic perturbation theory which was originally developed for chains of associating Lennard-Jones segments [7,8]. The SAFT approach in its various forms has been used successfully to examine the phase behaviour of a wide range of pure components, and of binary and ternary mixtures, and is now widely accepted as being one of the most powerful predictive tools in the description of the phase equilibria for both pure fluids and mixtures (see Ref. [5] for a brief overview). SAFT-VR is a recent extension to the original SAFT approach that treats potentials of variable attractive range, such as the square-well potential which has been used in this work. A more accurate description of the thermodynamics due to dispersion forces is used rather than a mean-field treatment of simpler versions of the theory such as SAFT-HS [9]. A greatly improved agreement between theoretical prediction of fluid phase equilibria and experimental data for non-associating systems is found [5,6,4,10]. In the SAFT-VR approach the *n*-alkanes are modeled as spherical segments tangentially bonded together to form chains. A simple empirical relationship [9,11] is used to determine the number of segments m representing each alkane molecule in terms of the number of carbon atoms C: $m = \frac{1}{3}(C-1)+1$, thus for methane $m = 1$ and for *n*-butane $m = 2$. The parameters for the pure components are obtained from a fit to the experimental vapour pressure and saturated liquid density data; the optimised parameters can then be re-scaled to the experimental critical point of each pure component. This is done to achieve better agreement between theoretical predictions and experimental data in the critical region; it should be noted that this is at the cost of poorer agreement with experimental data as we move farther away from the critical region. The simple Lorentz–Berthelot combining rules are used for the cross-interaction terms in the mixture calculation. For system II the theoretical parameters obtained in this way for the methane + *n*-butane binary mixture are used in the simulation study, so providing exact results for the model. Additionally the results of the simulations for both system I and II provide the first test for non-conformal systems of the mixing rules used in the SAFT-VR theory.

2. Gibbs ensemble Monte Carlo simulations

Here we shall present only a brief summary of the isothermal–isobaric GEMC method as applied to mixtures. For a more detailed description the reader is directed to the original papers [12,13].

In the GEMC simulation technique the coexisting vapour and liquid phases are monitored simultaneously in two distinct regions, a and b, with volumes V^a and V^b ($V = V^a + V^b$) and N^a and N^b particles, respectively ($N = N^a + N^b$). The two regions are not in physical contact but in thermodynamic equilibrium to satisfy the conditions of phase equilibrium: the equality of the pressure p, temperature T, and chemical potential μ of each species in both phases. A simulation cycle in the GEMC method consists of a combination of three distinct moves: N trial particle displacements (and re-orientations of the dimers) within each box to maintain the equality of temperature, one trial volume change of either subsystem a or b to maintain the equality of pressure, and a number of trial particle interchanges between the two subsystems to maintain the equality of the chemical potential, for which the particle transfer algorithm of Panagiotopoulos et al. [13] is used. The chemical potential is calculated using the Widom test particle method [14] as adapted to the GEMC technique [15]. The acceptance criterion is governed by a pseudo-Boltzmann factor, which for the *NPT* Gibbs ensemble method is given by [13]

$$\mathscr{P}^{\mathrm{Gibbs}} = \exp\left[\ln\left(\frac{N_1!}{N_1^a!N_1^b!}\right) + \ln\left(\frac{N_2!}{N_2^a!N_2^b!}\right) + N^a \ln V^a + N^b \ln V^b - \frac{pV^a}{kT} - \frac{pV^b}{kT} - \frac{E^a(N^a)}{kT} - \frac{E^b(N^b)}{kT}\right]. \quad (1)$$

where E^a and E^b are the energy of regions a and b, respectively, and k the Boltzmann constant. The maximum displacement and volume change is adjusted to give an acceptance ratio of between 30 and

40%, while the number of trial insertions are altered so that between 1 and 3% of particles are interchanged each cycle.

The systems we consider are binary mixtures of N_1 monomers and N_2 dimers. The monomers are modeled as square-well particles with hard spherical core of diameter σ and an attractive well of depth ε and range λ: the square-well potential (SW) is represented by

$$u_{ij}(r) = \begin{cases} +\infty & \text{if } r < \sigma_{ij}\,, \\ -\varepsilon_{ij} & \text{if } \sigma_{ij} \le r < \lambda_{ij}\sigma_{ij}\,, \\ 0 & \text{if } r \ge \lambda_{ij}\sigma_{ij}\,. \end{cases} \tag{2}$$

The homonuclear dimer particles are formed from tangentially bonded square-well segments. For system I the monomer and dimer segments have equal diameters and well depths ($\sigma = \sigma_{11} = \sigma_{22} = \sigma_{12}$ and $\varepsilon = \varepsilon_{11} = \varepsilon_{12} = \varepsilon_{22}$, respectively); the range of the square-well potential for the monomer segments is $\lambda_{11} = 1.25$, for the dimer segments $\lambda_{22} = 1.5$, and for the unlike interaction $\lambda_{12} = 1.375$. Computer simulations of the pure monomer and dimer systems have already been reported [16–18] and provide a test of our calculations by extrapolation of the mixture data to the pure component vapour pressure curves and coexisting densities. For system II the monomer and dimer segments have different segment sizes, depths and range of the attractive potential. The parameters from an earlier study of the binary system methane + *n*-butane using the SAFT-VR approach [4] are used in the simulation study ($\sigma_{22} = 1.074\sigma_{11}$, $\sigma_{12} = 1.037\sigma_{11}$, and $\varepsilon_{22} = 1.5309\varepsilon_{11}$, $\varepsilon_{12} = 1.2373\varepsilon_{11}$ with $\lambda_{11} = 1.494$ and $\lambda_{22} = 1.431$). The unlike size and energy parameters are obtained using the Lorentz–Berthelot combining rules and the cross range parameter is obtained from the arithmetic mean, $\lambda_{ij} = (\lambda_{ii}\sigma_{ii} + \lambda_{jj}\sigma_{jj})/(\sigma_{ii} + \sigma_{jj})$.

The majority of the simulations were performed with $N = 512$ particles. For state points that approach the critical region of the binary mixture a larger number of particles is needed; in this work we use $N = 1728$. In all the simulations the usual periodic boundary conditions (PBC) and minimum image convention (MIC) are applied. The initial guesses for the coexisting densities and compositions at a given temperature and pressure are obtained from the SAFT-VR predictions, details of which are given in the following section. After equilibrating the system for between 50 000 and 100 000 cycles, a further 150 000 to 250 000 cycles are carried out to accumulate the averages in order to determine the properties of the two coexisting phases.

3. SAFT-VR equation of state

The general equation for mixtures of chain molecules formed from hard-core segments with attractive interactions are given. For full details the reader is directed to the original papers [5,6].

The Helmholtz free energy A for an n-component mixture of chain molecules can be separated into the various contributions as

$$\frac{A}{NkT} = \frac{A^{\mathrm{IDEAL}}}{NkT} + \frac{A^{\mathrm{MONO}}}{NkT} + \frac{A^{\mathrm{CHAIN}}}{NkT}\,. \tag{3}$$

We should note the contribution due to association is not included since we are dealing with non-associating systems.

The ideal contribution to the free energy is given by a sum over all species i in the mixture [19],

$$\frac{A^{\mathrm{IDEAL}}}{NkT} = \left(\sum_{i=1}^{n} x_i \ln \rho_i \Lambda_i^3\right) - 1\,, \tag{4}$$

where $x_i = N_i/N$ is the mole fraction, $\rho_i = N_i/V$ the molecular number density, N_i the number of molecules, and Λ_i the thermal de Broglie wavelength of species i.

We can express the monomer Helmholtz free energy in terms of the free energy per monomer a^{M},

$$\frac{A^{\mathrm{MONO}}}{NkT} = \left(\sum_{i=1} x_i m_i\right)\frac{A^{\mathrm{M}}}{N_{\mathrm{s}}kT} = \left(\sum_{i=1} x_i m_i\right) a^{\mathrm{M}}\,, \tag{5}$$

where m_i is the number of spherical segments of chain i ($m_1 = 1$ for the monomer and $m_2 = 2$ for the dimer), and $N_{\mathrm{s}} = N_1 + 2N_2$ represents the total number of segments. Using the Barker and Henderson [20,21] perturbation theory for mixtures with a hard-sphere reference system the monomer free energy per segment is obtained from the expansion,

$$a^{\mathrm{M}} = a^{\mathrm{HS}} + \beta a_1 + \beta^2 a_2\,, \tag{6}$$

where $\beta = 1/kT$ and each term is now for a mixture of square-well spherical segments. The expression of Boublík [22] and Mansoori et al. [23] for a multicomponent mixture of hard spheres is used for the reference hard-sphere term,

$$a^{\mathrm{HS}} = \frac{6}{\pi\rho_{\mathrm{s}}}\left[\left(\frac{\zeta_2^3}{\zeta_3^2} - \zeta_0\right)\ln(1-\zeta_3) + \frac{3\zeta_1\zeta_2}{(1-\zeta_3)} + \frac{\zeta_2^3}{\zeta_3(1-\zeta_3)^2}\right], \quad (7)$$

where $\rho_{\mathrm{s}} = N_{\mathrm{s}}/V$ is the total number density of spherical segments, and ζ_l are the reduced densities defined by

$$\zeta_l = \frac{\pi\rho_{\mathrm{s}}}{6}\left[\sum_{i=1}^{n} x_{\mathrm{s},i}\sigma_{ii}^l\right], \quad (8)$$

where $x_{\mathrm{s},i}$ is the mole fraction of segments of type i in the mixture. For the evaluation of the perturbative terms a_1 and a_2 we have used the van der Waals one (VDW-1) fluid approximation (see Ref. [6] for more details). The mean attractive energy represented by the a_1 term is obtained from the sum of the partial terms corresponding to each type of pair interaction, which are written in terms of the contact values of g_{ij}^{HS} using the mean-value theorem,

$$a_1 = \sum_{i=1}^{n}\sum_{j=1}^{n} x_{\mathrm{s},i}x_{\mathrm{s},j}a_1^{ij} = -\rho_{\mathrm{s}}\sum_i\sum_j x_{\mathrm{s},i}x_{\mathrm{s},j}\alpha_{ij}^{\mathrm{VDW}}g_{ij}^{\mathrm{HS}}\left[\sigma_{ij};\zeta_3^{\mathrm{eff}}\right], \quad (9)$$

where

$$\alpha_{ij}^{\mathrm{VDW}} = 2\pi\varepsilon_{ij}\sigma_{ij}^3\left(\lambda_{ij}^3 - 1\right)/3 \quad (10)$$

is the van der Waals attractive constant for the i–j interaction, and ζ_3^{eff} is an effective packing fraction.

In the VDW-1 fluid theory g_{ij}^{HS} (those which appear in the perturbative terms only) is approximated by the radial distribution function for a single fluid so that Eq. (9) simplifies to

$$a_1 = -\rho_{\mathrm{s}}\sum_i\sum_j x_{\mathrm{s},i}x_{\mathrm{s},j}\alpha_{ij}^{\mathrm{VDW}}g_0^{\mathrm{HS}}\left[\sigma_{\mathrm{x}};\zeta_{\mathrm{x}}^{\mathrm{eff}}\right], \quad (11)$$

where g_0^{HS} is the contact value of the hard-sphere pair radial distribution obtained from the Carnahan and Starling equation of state [24],

$$g_0^{\mathrm{HS}}\left[\sigma_{\mathrm{x}};\zeta_{\mathrm{x}}^{\mathrm{eff}}\right] = \frac{1-\zeta_{\mathrm{x}}^{\mathrm{eff}}/2}{\left(1-\zeta_{\mathrm{x}}^{\mathrm{eff}}\right)^3}. \quad (12)$$

The effective packing fraction $\zeta_{\mathrm{x}}^{\mathrm{eff}}$ in Eq. (12) is obtained, within the VDW-1 fluid approximation, from the corresponding packing fraction of the mixture ζ_{x}:

$$\zeta_{\mathrm{x}}^{\mathrm{eff}}\left(\zeta_{\mathrm{x}},\lambda_{ij}\right) = c_1\left(\lambda_{ij}\right)\zeta_{\mathrm{x}} + c_2\left(\lambda_{ij}\right)\zeta_{\mathrm{x}}^2 + c_3\left(\lambda_{ij}\right)\zeta_{\mathrm{x}}^3, \quad (13)$$

where

$$\zeta_{\mathrm{x}} = \frac{\pi}{6}\rho_{\mathrm{s}}\sum_i\sum_j x_{\mathrm{s},i}x_{\mathrm{s},j}\sigma_{ij}^3 = \frac{\pi}{6}\rho_{\mathrm{s}}\sigma_{\mathrm{x}}^3, \quad (14)$$

with

$$\sigma_{\mathrm{x}}^3 = \sum_i\sum_j x_{\mathrm{s},i}x_{\mathrm{s},j}\sigma_{ij}^3. \quad (15)$$

The coefficients c_1, c_2 and c_3 are approximated by those of the pure fluid [5,6],

$$\begin{pmatrix} c_1 \\ c_2 \\ c_3 \end{pmatrix} = \begin{pmatrix} 2.25855 & -1.50349 & 0.249434 \\ -0.669270 & 1.40049 & -0.827739 \\ 10.1576 & -15.0427 & 5.30827 \end{pmatrix} \times \begin{pmatrix} 1 \\ \lambda_{ij} \\ \lambda_{ij}^2 \end{pmatrix}. \quad (16)$$

This corresponds to the MX1b mixing rule of Ref. [6]. We use the VDW-1 fluid mixing rule rather than the actual packing fraction of the system ζ_3 in order to evaluate ζ_3^{eff} (MX3b mixing rule) since the slices of the phase diagram that we have studied are in the critical region (see Refs. [5,10]).

The first fluctuation term of the free energy a_2 is written in terms of a_1 within the local compressibility approximation,

$$a_2 = \sum_{i=1}^{n}\sum_{j=1}^{n} x_{\mathrm{s},i}x_{\mathrm{s},j}\frac{1}{2}K^{\mathrm{HS}}\varepsilon_{ij}\rho_{\mathrm{s}}\frac{\partial a_1^{ij}}{\partial\rho_{\mathrm{s}}}, \quad (17)$$

where K^{HS} is the hard-sphere isothermal compressibility of Percus-Yevick [25]

$$K^{\mathrm{HS}} = \frac{\zeta_0(1-\zeta_3)^4}{\zeta_0(1-\zeta_3)^2 + 6\zeta_1\zeta_2(1-\zeta_3) + 9\zeta_2^3}. \quad (18)$$

Finally, the contribution to the free energy due to chain formation is expressed in terms of the contact value of the background correlation function,

$$\frac{A_{\mathrm{CHAIN}}}{NkT} = -\sum_{i=1}^{n} x_i(m_i - 1)\ln y_{ii}^{\mathrm{SW}}(\sigma_{ii}), \qquad (19)$$

where $y_{ii}^{\mathrm{SW}}(\sigma_{ii}) = g_{ii}^{\mathrm{SW}}(\sigma_{ii})\exp(-\beta\varepsilon_{ii})$. We obtain $y_{ii}^{\mathrm{SW}}(\sigma_{ii})$ from the high-temperature expansion of $g_{ii}^{\mathrm{SW}}(\sigma_{ii})$,

$$g_{ii}^{\mathrm{SW}}(\sigma_{ii}) = g_{ii}^{\mathrm{HS}}(\sigma_{ii}) + \beta\varepsilon_{ii}g_1(\sigma_{ii}). \qquad (20)$$

At this point we remind the reader that only the hard-sphere expressions of the perturbative terms are evaluated within the VDW-1 fluid approximation, and therefore g_{ii}^{HS} is evaluated in full using the expression of Boublík [22],

$$g_{ij}^{\mathrm{HS}}(\sigma_{ij};\zeta_3) = \frac{1}{1-\zeta_3} + 3\frac{D_{ij}\zeta_3}{(1-\zeta_3)^2} + 2\frac{(D_{ij}\zeta_3)^2}{(1-\zeta_3)^3}, \qquad (21)$$

with the parameter D_{ij} defined by

$$D_{ij} = \frac{\sigma_{ii}\sigma_{jj}}{\sigma_{ii}+\sigma_{jj}}\frac{\sum_{i=1}^{n} x_{\mathrm{s},i}\sigma_{ii}^2}{\sum_{i=1}^{n} x_{\mathrm{s},i}\sigma_{ii}^3}. \qquad (22)$$

The term $g_1(\sigma_{ii})$ is obtained from a self-consistent method for the pressure p from the Clausius virial theorem and from the density derivative of the Helmholtz free energy giving

$$g_1^{ij}(\sigma_{ij}) = \frac{1}{2\pi\varepsilon_{ij}\sigma_{ij}^3}\left[3\left(\frac{\partial a_1^{ij}}{\partial\rho_{\mathrm{s}}}\right) - \frac{\lambda_{ij}}{\rho_{\mathrm{s}}}\frac{\partial a_1^{ij}}{\partial\lambda_{ij}}\right], \qquad (23)$$

and so using Eq. (11) we obtain

$$g_1(\sigma_{ii};\zeta_3) = g_0^{\mathrm{HS}}\left[\sigma_{\mathrm{x}};\zeta_{\mathrm{x}}^{\mathrm{eff}}\right] + \left(\lambda_{ii}^3 - 1\right)\frac{\partial g_0^{\mathrm{HS}}\left[\sigma_{\mathrm{x}};\zeta_{\mathrm{x}}^{\mathrm{eff}}\right]}{\partial\zeta_{\mathrm{x}}^{\mathrm{eff}}} \times\left(\frac{\lambda_{ii}}{3}\frac{\partial\zeta_{\mathrm{x}}^{\mathrm{eff}}}{\partial\lambda_{ii}} - \zeta_3\frac{\partial\zeta_{\mathrm{x}}^{\mathrm{eff}}}{\partial\zeta_3}\right), \qquad (24)$$

where g_0^{HS} is evaluated within the VDW-1 fluid theory. Using standard thermodynamic relationships other thermodynamic properties can be obtained from the Helmholtz free energy such as the chemical potential,

$$\mu_i = \left(\frac{\partial A}{\partial N_i}\right)_{T,V,N_{j\neq i}}, \qquad (25)$$

and the compressibility factor

$$Z = \frac{pV}{NkT} = \sum_i\left(x_i\frac{\mu_i}{kT}\right) - \frac{A}{NkT}. \qquad (26)$$

These are the functions required for the determination of the critical and phase behaviour of the mixture. The gas–liquid and liquid–liquid critical lines can be determined by equating the second and third derivatives of the Gibbs free energy with re-

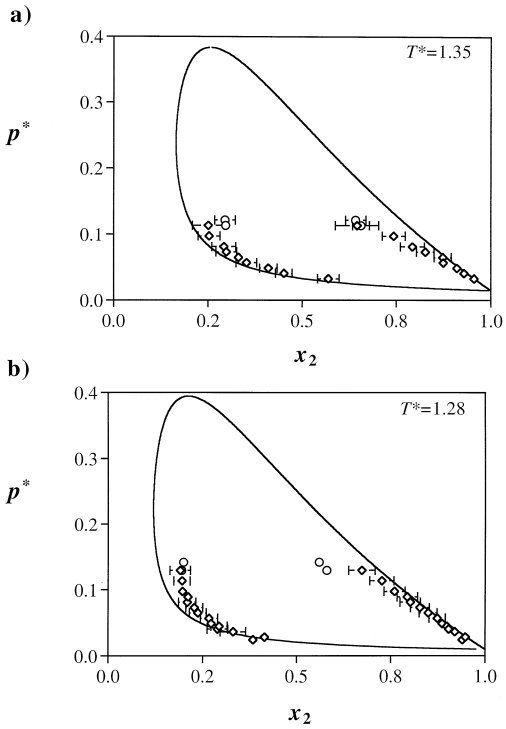

Fig. 1. Pressure–composition slices of the vapour–liquid coexistence for the square-well monomer(1)–dimer(2) mixture of system I. The reduced pressure is given by $P^* = P\sigma^3/\varepsilon$, the reduced temperature $T^* = kT/\varepsilon$ and x_2 is the mole fraction of dimers. The diamonds and circles represent the results of the GEMC simulations for systems of $N = 512$ and $N = 1728$ particles, respectively, and the continuous curves correspond to the SAFT-VR prediction.

Table 1
Vapour–liquid coexistence data obtained from *NPT* Gibbs ensemble Monte Carlo simulations for a square-well monomer–dimer mixture with fixed variables: $\sigma_{22} = 1.00\sigma_{11}$, $\varepsilon_{22} = 1.00\varepsilon_{11}$, and $\lambda_1 = 1.25$, $\lambda_2 = 1.5$. $N = 512$, the reduced pressure $P^* = P\sigma^3/\varepsilon$ and the reduced temperature $T^* = kT/\varepsilon = 1.28$. The packing fractions ζ_3, dimer mole fractions x_2, and the reduced energies per segment $E^* = E/\varepsilon N_s$ in the coexisting vapour and liquid phases are labelled v and l, respectively. The uncertainties correspond to one standard deviation. Results labelled with a † are obtained using $N = 1728$ particles

P^*	$x_{2,v}$	$x_{2,l}$	$\zeta_{3,v}$	$\zeta_{3,l}$	E_v^*	E_l^*
0.024	0.384 ± 0.021	0.940 ± 0.016	0.021 ± 0.001	0.339 ± 0.009	−0.358 ± 0.054	−4.312 ± 0.121
0.041	0.290 ± 0.028	0.904 ± 0.018	0.024 ± 0.002	0.338 ± 0.010	−0.356 ± 0.057	−4.160 ± 0.127
0.049	0.273 ± 0.021	0.886 ± 0.020	0.029 ± 0.002	0.330 ± 0.010	−0.415 ± 0.060	−4.158 ± 0.129
0.057	0.267 ± 0.023	0.873 ± 0.022	0.033 ± 0.003	0.332 ± 0.010	−0.477 ± 0.067	−4.173 ± 0.131
0.065	0.237 ± 0.023	0.849 ± 0.024	0.037 ± 0.002	0.330 ± 0.010	−0.504 ± 0.066	−4.131 ± 0.137
0.073	0.228 ± 0.022	0.827 ± 0.025	0.042 ± 0.003	0.327 ± 0.010	−0.559 ± 0.071	−4.073 ± 0.134
0.081	0.209 ± 0.023	0.802 ± 0.027	0.046 ± 0.003	0.322 ± 0.012	−0.582 ± 0.073	−3.997 ± 0.152
0.089	0.212 ± 0.019	0.794 ± 0.027	0.051 ± 0.004	0.325 ± 0.012	−0.647 ± 0.082	−4.024 ± 0.141
0.097	0.196 ± 0.021	0.760 ± 0.028	0.055 ± 0.005	0.318 ± 0.014	−0.679 ± 0.083	−3.914 ± 0.150
0.113	0.195 ± 0.022	0.727 ± 0.032	0.065 ± 0.004	0.314 ± 0.011	−0.792 ± 0.095	−3.848 ± 0.171
0.130	0.191 ± 0.027	0.673 ± 0.035	0.075 ± 0.006	0.302 ± 0.017	−0.889 ± 0.109	−3.663 ± 0.194
0.130†	0.194 ± 0.019	0.580 ± 0.018	0.078 ± 0.004	0.241 ± 0.014	−0.933 ± 0.070	−3.114 ± 0.125
0.142†	0.199 ± 0.017	0.559 ± 0.018	0.088 ± 0.004	0.246 ± 0.011	−1.047 ± 0.078	−3.102 ± 0.108

spect to the mole fraction to zero. Phase equilibrium between phases a and b in mixtures requires that the temperature, pressure, and chemical potential of each component in each phase be equal [26],

$$T^a = T^b\,, \quad P^a = P^b\,, \quad \mu_i^a = \mu_i^b\,. \tag{27}$$

These conditions are solved numerically using a simplex method [27].

4. Results

We have examined through SAFT-VR theory and GEMC simulation the phase equilibria of the two square-well monomer–dimer binary systems. In our discussion of the results the usual reduced thermodynamic variables have been used: $\rho^* = N\sigma_{11}^3/V$ for the density, ζ_3 for the packing fraction (η for pure components), $T^* = kT/\varepsilon_{11}$ for the temperature and

Table 2
Vapour–liquid coexistence data obtained from *NPT* Gibbs ensemble Monte Carlo simulations for a square-well monomer–dimer mixture at a reduced temperature of $T^* = 1.35$. Results labelled with a † are obtained using $N = 1728$ particles. See Table 1 for details

P^*	$x_{2,v}$	$x_{2,l}$	$\zeta_{3,v}$	$\zeta_{3,l}$	E_v^*	E_l^*
0.032	0.570 ± 0.029	0.956 ± 0.013	0.024 ± 0.002	0.320 ± 0.010	−0.468 ± 0.068	−4.058 ± 0.130
0.041	0.451 ± 0.022	0.929 ± 0.018	0.027 ± 0.002	0.313 ± 0.013	−0.462 ± 0.067	−3.967 ± 0.160
0.049	0.410 ± 0.023	0.910 ± 0.018	0.031 ± 0.002	0.312 ± 0.012	−0.511 ± 0.073	−3.942 ± 0.141
0.057	0.352 ± 0.028	0.874 ± 0.021	0.036 ± 0.003	0.302 ± 0.013	−0.545 ± 0.082	−3.802 ± 0.150
0.065	0.331 ± 0.021	0.873 ± 0.023	0.038 ± 0.003	0.311 ± 0.012	−0.423 ± 0.031	−3.891 ± 0.149
0.073	0.298 ± 0.028	0.827 ± 0.024	0.043 ± 0.004	0.292 ± 0.015	−0.597 ± 0.081	−3.662 ± 0.159
0.081	0.292 ± 0.032	0.793 ± 0.032	0.049 ± 0.005	0.278 ± 0.021	−0.668 ± 0.104	−3.500 ± 0.216
0.097	0.253 ± 0.029	0.743 ± 0.030	0.054 ± 0.004	0.267 ± 0.019	−0.595 ± 0.092	−3.346 ± 0.192
0.113	0.250 ± 0.042	0.646 ± 0.058	0.066 ± 0.008	0.229 ± 0.036	−0.710 ± 0.175	−2.917 ± 0.365
0.113†	0.297 ± 0.020	0.657 ± 0.022	0.070 ± 0.004	0.216 ± 0.015	−0.944 ± 0.077	−2.922 ± 0.146
0.122†	0.295 ± 0.027	0.643 ± 0.027	0.080 ± 0.005	0.228 ± 0.019	−1.051 ± 0.104	−2.982 ± 0.176

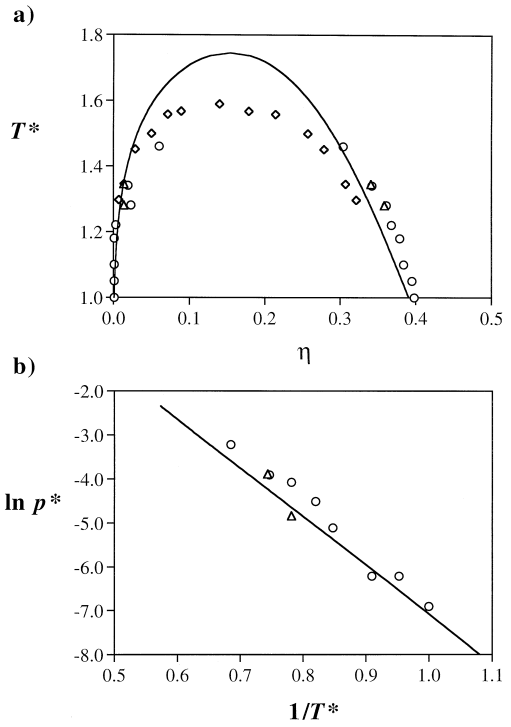

Fig. 2. (a) Vapour–liquid coexistence densities and (b) vapour pressures for the square-well dimer with $\lambda = 1.5$. $T^* = kT/\varepsilon$ and $\eta = \pi\rho_s\sigma^3/6$ is the packing fraction. The triangles and circles represent the results obtained by extrapolating GEMC mixture data in this work and that of Davies et al. [18], respectively, the diamonds to the GEMC data of Yethiraj and Hall [16] and the continuous curves the SAFT-VR prediction.

$P^* = P\sigma_{11}^3/\varepsilon_{11}$ for the pressure. The compositions of the monomer (component 1) and the dimer (component 2) are denoted by $x_1 = N_1/N$ and $x_2 = N_2/N$, respectively. System I provided a test of the non-conformal aspect of the theory and was a natural next step on from previous work on conformal monomer–dimer fluid systems [18], as we are able to examine the direct effect of different ranges of potential on the phase equilibria of the system. *Px* slices of the vapour–liquid phase diagram were examined at $T^* = 1.28$ and $T^* = 1.35$ which are shown in Fig. 1a and b, respectively. Both slices are supercritical as we are above the critical point of the more volatile pure component ($T_{1,c}^* = 0.764$ and $P_{1,c}^* = 0.081$ [17]). The simulation results for the mole fractions, densities and energies of the coexisting vapour and liquid phases are summarised in Tables 1 and 2. We see good agreement between the theory and exact simulation data at low pressures although a deviation is seen at higher pressures. This is an unavoidable feature of the description of critical behaviour with equations of state which are based on analytical expressions for the free energy and has been discussed in earlier work [5]. Comparisons can be drawn between the results presented here and those of a similar study by Davies et al. [18]. In both studies the monomer and dimer segments have equal diameters and well depths, the work of Davies et al. being for a conformal system with $\lambda_{11} = \lambda_{22} = 1.5$ while the present work for a non-conformal system

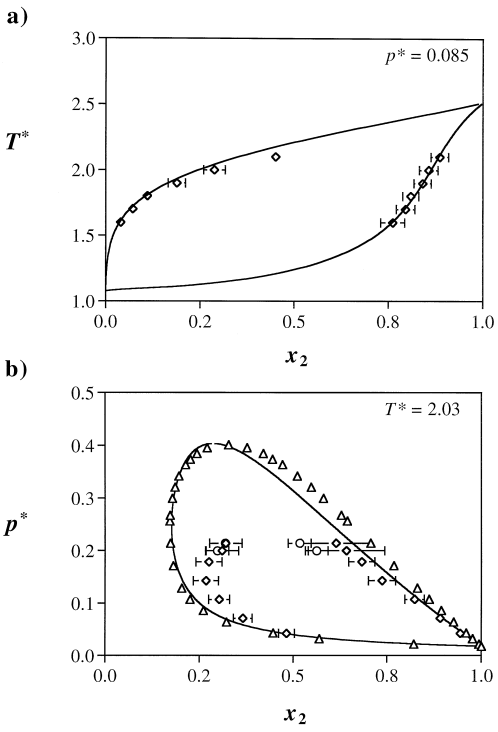

Fig. 3. (a) Pressure–composition and (b) temperature–composition slices of the vapour–liquid coexistence for the square-well monomer(1)–dimer(2) mixture of system II. The reduced pressure is given by $P^* = P\sigma_{11}^3/\varepsilon_{11}$, the reduced temperature $T^* = kT/\varepsilon_{11}$ and x_2 is the mole fraction of dimers. The diamonds and circles represent the results of the GEMC simulations for systems of $N = 512$ and $N = 1728$ particles, respectively, the triangles the methane + butane experimental data of Kahre et al. [28], and the continuous curves correspond to the SAFT-VR prediction.

Table 3
Vapour–liquid coexistence data obtained from *NPT* Gibbs ensemble Monte Carlo simulations for a square-well monomer–dimer mixture with fixed variables: $\sigma_{22} = 1.074\sigma_{11}$, $\varepsilon_{22} = 1.5309\varepsilon_{11}$, and $\lambda_1 = 1.431$, $\lambda_2 = 1.494$. $N = 512$, the reduced pressure $P^* = P\sigma_{11}^3/\varepsilon_{11} = 0.085$ and the reduced temperature $T^* = kT/\varepsilon_{11}$. The packing fractions ζ_3, dimer mole fractions x_2, and the reduced energies per segment $E^* = E/\varepsilon_{11}N_s$ in the coexisting vapour and liquid phases are labelled v and l, respectively. The uncertainties correspond to one standard deviation

T^*	$x_{2,v}$	$x_{2,l}$	$\zeta_{3,v}$	$\zeta_{3,l}$	E_v^*	E_l^*
1.600	0.040 ± 0.012	0.762 ± 0.031	0.033 ± 0.002	0.371 ± 0.008	−0.513 ± 0.068	−7.027 ± 0.193
1.700	0.072 ± 0.016	0.796 ± 0.025	0.032 ± 0.002	0.360 ± 0.007	−0.526 ± 0.074	−6.835 ± 0.169
1.800	0.110 ± 0.018	0.810 ± 0.021	0.032 ± 0.003	0.344 ± 0.007	−0.550 ± 0.084	−6.509 ± 0.147
1.900	0.188 ± 0.023	0.841 ± 0.023	0.034 ± 0.003	0.333 ± 0.009	−0.656 ± 0.099	−6.300 ± 0.180
2.000	0.288 ± 0.029	0.857 ± 0.024	0.037 ± 0.003	0.314 ± 0.012	−0.804 ± 0.116	−5.941 ± 0.234
2.100	0.451 ± 0.021	0.887 ± 0.023	0.046 ± 0.004	0.300 ± 0.015	−1.126 ± 0.138	−5.690 ± 0.276

with $\lambda_{11} = 1.25$ and $\lambda_{22} = 1.5$. The two systems thus only differ in the range of the attractive potential of the monomer species, which in turn leads to a differing unlike range parameter ($\lambda_{12} = 1.375$). The results presented here show a slight negative deviation from Raoult's law as do those of the conformal system although the two phase regions are wider in composition.

In addition to providing us with information on the phase behaviour of the mixture the simulation data can be used to yield an estimate of the pure component vapour–liquid equilibria. Extrapolation of the *Px* slices using a Raoult's law dependence close to the dimer axis ($x_2 = 1$ and $x_1 = 0$) yields vapour–liquid coexistence points, and extrapolating the temperature density data of the mixture provides coexisting density data. Both agree well with previously reported results as can be seen in Fig. 2, where we compare the coexisting densities and vapour pressures of this work with earlier studies [16,18] and the SAFT-VR prediction.

For system II both a *Px* slice and a *Tx* slice have been examined (see Fig. 3a and b). The simulation results for the mole fractions, densities and energies of the coexisting vapour and liquid phases are reported in Tables 3 and 4. The subcritical constant-pressure slice at $P^* = 0.085$ shows very good agreement between the theoretical prediction and computer simulation results. The constant-temperature slice shown in Fig. 3b is clearly supercritical as the coexistence envelope ends in a gas–liquid critical point and not at the monomer pure component axis. The exact simulation results are in good agreement with the theoretical prediction away from the critical

Table 4
Vapour–liquid coexistence data obtained from *NPT* Gibbs ensemble Monte Carlo simulations for a square-well monomer–dimer mixture at a reduced temperature of $T^* = 2.03$. Results labelled with a † are obtained using $N = 1728$ particles. See Table 3 for details

P^*	$x_{2,v}$	$x_{2,l}$	$\zeta_{3,v}$	$\zeta_{3,l}$	E_v^*	E_l^*
0.042	0.482 ± 0.021	0.944 ± 0.014	0.022 ± 0.002	0.314 ± 0.010	−0.608 ± 0.095	−6.034 ± 0.208
0.071	0.366 ± 0.025	0.891 ± 0.020	0.033 ± 0.003	0.309 ± 0.012	−0.777 ± 0.114	−5.875 ± 0.225
0.107	0.303 ± 0.028	0.823 ± 0.026	0.049 ± 0.004	0.302 ± 0.014	−1.027 ± 0.144	−5.680 ± 0.251
0.142	0.268 ± 0.033	0.737 ± 0.036	0.063 ± 0.006	0.280 ± 0.021	−1.230 ± 0.183	−5.212 ± 0.347
0.178	0.284 ± 0.030	0.692 ± 0.037	0.084 ± 0.009	0.276 ± 0.019	−1.594 ± 0.230	−5.069 ± 0.322
0.199	0.311 ± 0.044	0.642 ± 0.102	0.102 ± 0.016	0.265 ± 0.050	−1.975 ± 0.366	−4.888 ± 0.817
0.199†	0.298 ± 0.030	0.563 ± 0.030	0.103 ± 0.009	0.222 ± 0.017	−1.977 ± 0.233	−4.197 ± 0.256
0.213	0.320 ± 0.043	0.614 ± 0.093	0.115 ± 0.015	0.260 ± 0.046	−2.197 ± 0.357	−4.750 ± 0.763
0.213†	0.319 ± 0.020	0.517 ± 0.030	0.118 ± 0.008	0.207 ± 0.015	−2.245 ± 0.181	−3.916 ± 0.258

region, and the discrepancy at higher pressures is consistent with that observed for system I (Fig. 1). Although the same parameters were used in the simulation and theoretical study of the model methane + *n*-butane system better agreement is observed between theory and the experimental data [28]. This is expected as the parameters for the models are chosen by fitting to the experimental saturated liquid densities and vapour pressures of the pure components with simple Lorentz–Berthelot combining rules for the cross interaction terms. In order to improve the theoretical description of the critical region an accurate treatment of non-classical critical behaviour is needed, such as those of Prausnitz or Sengers and co-workers [29,30].

5. Conclusions

We have presented GEMC simulation results for the phase equilibrium of two non-conformal monomer–dimer systems and compared the results of the SAFT-VR approach. SAFT is a molecular based equation of state enabling each term to be directly tested by computer simulation, which enables improvement of the theory. For the systems studied good agreement between theory and simulation is seen and the over-prediction of the critical region by the theory is highlighted. The results presented also provided a test of the MX1b mixing rule used in the SAFT-VR theory for non-conformal systems.

Although SAFT-VR has successfully been used to treat a wide range of experimental systems (alkanes, perfluoroalkanes and their mixtures [5,4,10,31], refrigerant systems [32], hydrogen chloride and alkanes [33], etc.) a more accurate treatment of the critical region is needed. This problem is common to all analytical van der Waals type equations of state and special methods are required to incorporate the non-classical critical behaviour.

Acknowledgements

CMcC thanks Sheffield University for a UGC scholarship, AGV thanks the EPSRC and the ICI Strategic Research Fund for funding Research Fellowships. We also acknowledge support from the European Commission (CI1*-CT94-0132), the Royal Society, and the Computational and ROPA Initiatives of the EPSRC for funding.

References

[1] A.Z. Panagiotopoulos, Mol. Simul. 9 (1992) 1.
[2] A.Z. Panagiotopoulos, M.R. Stapleton, Fluid Phase Equilib. 53 (1989) 133.
[3] K.E. Gubbins, Mol. Simul. 2 (1989) 223.
[4] C. McCabe, A. Galindo, A. Gil-Villegas, G. Jackson, Int. J. Thermophys. 19 (1998) 1511.
[5] A. Gil-Villegas, A. Galindo, P.J. Whitehead, S.J. Mills, G. Jackson, A.N. Burgess, J. Chem. Phys. 106 (1997) 4168.
[6] A. Galindo, L.A. Davies, A. Gil-Villegas, G. Jackson, Mol. Phys. 93 (1998) 241.
[7] W.G. Chapman, K.E. Gubbins, G. Jackson, M. Radosz, Fluid Phase Equilib. 52 (1989) 31.
[8] W.G. Chapman, K.E. Gubbins, G. Jackson, M. Radosz, Ind. Eng. Chem. Res. 29 (1990) 1709.
[9] A. Galindo, P.J. Whitehead, G. Jackson, A.N. Burgess, J. Phys. Chem. 100 (1996) 6781.
[10] C. McCabe, A. Gil-Villegas, G. Jackson, J. Phys. Chem. B 102 (1998) 4183.
[11] G. Jackson, K.E. Gubbins, Pure Appl. Chem. 61 (1989) 1021.
[12] A.Z. Panagiotopoulos, Mol. Phys. 61 (1987) 813.
[13] A.Z. Panagiotopoulos, N. Quirke, M.R. Stapleton, D.J. Tildesley, Mol. Phys. 63 (1988) 527.
[14] B. Widom, J. Chem. Phys. 39 (1963) 2808.
[15] B. Smit, D. Frenkel, Mol. Phys. 68 (1989) 951.
[16] A. Yethiraj, C.K. Hall, Mol. Phys. 72 (1991) 619.
[17] L. Vega, E. de Miguel, L.F. Rull, G. Jackson, I.A. McLure, J. Chem. Phys. 96 (1992) 2296.
[18] L.A. Davies, A. Gil-Villegas, G. Jackson, S. Calero, S. Lago, Phys. Rev. E. 55 (1998) 2035.
[19] J.P. Hansen, I.R. McDonald, Theory of Simple Liquids, 2nd ed., Academic Press, London, 1986.
[20] P.J. Leonard, D. Henderson, J.A. Barker, Trans. Faraday Soc. 66 (1970) 2439.
[21] J.A. Barker, D. Henderson, Rev. Mod. Phys. 48 (1976) 587.
[22] T.J. Boublík, J. Chem. Phys. 53 (1970) 471.
[23] G.A. Mansoori, N.F. Carnahan, K.E. Starling, T.W. Leland, J. Chem. Phys. 54 (1971) 1523.
[24] N.F. Carnahan, K.E. Starling, J. Chem. Phys. 51 (1969) 635.
[25] T.M. Reid, K.E. Gubbins, Applied Statistical Mechanics, McGraw-Hill, Tokyo, 1973.
[26] J.S. Rowlinson, F.L. Swinton, Liquids and Liquid Mixtures, 3rd ed., Butterworth, London, 1982.
[27] W.H. Press, S.A. Teukolsky, W.T. Vetterling, B.P. Flannery, Numerical Recipes in Fortran, 1st ed., Cambridge University Press, Cambridge, 1986.
[28] L.C. Kahre, J. Chem. Eng. Data 19 (1974) 67.

[29] L. Lue, J.M. Prausnitz, J. Chem. Phys. 108 (1998) 5529.
[30] A. van Pelt, G.X. Jin, J.V. Sengers, Int. J. Thermophys. 15 (1994) 687.
[31] C. McCabe, A. Galindo, A. Gil-Villegas, G. Jackson, J. Phys. Chem. 102 (1998) 8060.
[32] A. Galindo, A. Gil-Villegas, P.J. Whitehead, A.N. Burgess, G. Jackson, J. Chem. Phys. 102 (1998) 7632.
[33] A. Galindo, L.J. Florusse, C.J. Peters, Fluid Phase Equilib. (1998, accepted).